Published in final edited form as:
Neuron. 2012 March 8; 73(5): 990–1001. doi:10.1016/j.neuron.2011.12.036.

Distinct Neuronal Coding Schemes in Memory Revealed by Selective Erasure of Fast Synchronous Synaptic Transmission

Wei Xu[1,2], **Wade Morishita**[3], **Paul S. Buckmaster**[4], **Zhiping P. Pang**[2], **Robert C. Malenka**[3], and **Thomas C. Südhof**[1,2,*]

[1]Howard Hughes Medical Institute, Stanford University School of Medicine, Stanford, California 94305, USA

[2]Department of Molecular and Cellular Physiology, Stanford University School of Medicine, Stanford, California 94305, USA

[3]Nancy Pritzker Laboratory in the Department of Psychiatry and Behavioral Sciences, Stanford University School of Medicine, Stanford, California 94305, USA

[4]Department of Comparative Medicine, Stanford University School of Medicine, Stanford, California 94305, USA

Abstract

Neurons encode information by firing spikes in isolation or bursts, and propagate information by spike-triggered neurotransmitter release that initiates synaptic transmission. Isolated spikes trigger neurotransmitter release unreliably but with high temporal precision, whereas bursts of spikes boost transmission fidelity by overcoming the unreliability of spike-triggered release but are temporally imprecise. However, the relative physiological importance of different spike firing modes remains unclear. Here, we show that knockdown of synaptotagmin-1, the major Ca^{2+}-sensor for neurotransmitter release, abrogated neurotransmission evoked by isolated spikes, but only delayed without abolishing neurotransmission evoked by bursts of spikes. Nevertheless, knockdown of synaptotagmin-1 in the hippocampal CA1 region did not impede acquisition of recent contextual fear memories, although it did impair the precision of such memories. In contrast, knockdown of synaptotagmin-1 in the prefrontal cortex impaired all remote fear memories. These results indicate that different brain circuits and types of memory employ distinct spike-coding schemes to encode and transmit information.

INTRODUCTION

Neurons are thought to encode information in a continuum of firing patterns ranging from isolated spikes to high-frequency bursts of 2–20 spikes. In place cells of the CA1 region of the hippocampus, ~50% of spikes occur in short bursts with frequencies of >50 Hz, while the remaining spikes occur in isolation (Harris et al., 2001; Harvey et al., 2009; Jones and Wilson, 2005; Ranck, 1973). The occurrence of spike bursts varies with behavioral state (Burgos-Robles et al., 2007; Harris et al., 2001; Ranck, 1973), and is altered in neurological diseases (Jackson et al., 2004; Walker et al., 2008). These properties suggest that spike

*To whom correspondence should be addressed (tcs1@stanford.edu).

bursting patterns are functionally important for information processing by the brain, but the specific roles of spike firing patterns in behaviors remain largely unexplored.

Typically, central synapses exhibit a low probability of neurotransmitter release in response to a single spike, although each release event triggered by a spike is temporally precise (Borst, 2010; Branco and Staras, 2009). The low probability of neurotransmitter release renders single spike transmission unreliable, which may serve to provide a large dynamic range for plasticity, or to maximize the brain information storage capacity under resource constraints (Varshney et al., 2006). Neurons can use two strategies to overcome the unreliability of single spike transmission. They can either simultaneously activate multiple synapses connecting to the same target via isolated spikes, or repeatedly activate a single synapse via bursts of spikes (Lisman, 1997). Each of these two strategies incurs a tradeoff. Use of multiple synapses allows information to be transmitted by a single spike, thus ensuring high speed, temporal precision, and strength, but at the cost of a reduced capacity for storing and processing information (Varshney et al., 2006). Some synapses in sensory transduction or motor control pathways choose this strategy, for example the calyx of Held synapse in the auditory pathway which forms more than 500 release sites on its target neuron (Meyer et al., 2001), or climbing fibers in the cerebellum which form multiple synapses on a single Purkinje cell (Silver et al., 1998). Conversely, use of burst-mediated transmission requires only one or a few synapses for high-fidelity transmission, but reduces the temporal resolution of transmission, as for example observed in inhibitory interneurons (Sheffield et al., 2011). Therefore this mode of firing may be better suited for neurons involved in the storage of large amounts of information. Bursts may also play roles in the organization of neuronal assemblies and dendritic local integration (Izhikevich et al., 2003; Polsky et al., 2009).

Although firing of isolated spikes and bursts of spikes as the two principal modes of information coding have long been recognized, their relative importance in a particular neuronal circuit has been difficult to test experimentally, especially in behaving animals, because no approach to selectively shut down one or the other mode of synaptic transmission was available. Here, we show that synaptic transmission triggered by isolated spikes can be selectively ablated using knockdown (KD) of synaptotagmin-1 (Syt1), the major Ca^{2+}-sensor for synchronous neurotransmitter release (Geppert et al., 1994). However, as in Syt1 knockout mice (Maximov and Südhof, 2005), the Syt1 KD does not abolish release in response to bursts of spikes. Instead, the Syt1 KD shifts the timing of release induced by a high-frequency action potential train into a delayed, non-physiological mode because the massive influx of Ca^{2+} into nerve terminals induced by a high-frequency action potential train activates asynchronous release that is normally suppressed by the presence of Syt1 (Maximov and Südhof, 2005). Thus, the Syt1 KD allows us to specifically impair information transfer that is mediated by isolated spikes or that requires precise timing of burst of spikes, and to test the effects of such manipulations on fear memories as a model behavior. In this procedure, we are not interfering with spike firing itself, but with the transmission of signals originating by these spikes. Unexpectedly, we find that transmission of the information by isolated spikes is dispensable for acquisition of recent contextual memories via the hippocampus, although it is essential for memory function by the medial prefrontal cortex.

RESULTS

The Syt1 KD institutes a high-pass frequency filter for synaptic transmission

We analyzed cultured cortical neurons that were infected with lentiviruses expressing a Syt1 shRNA (Syt1 KD) or tetanus-toxin light chain (TetTox), and recorded inhibitory postsynaptic currents (IPSCs; Maximov et al., 2007; Pang et al., 2010; for KD efficiency

and specificity, see Figs. S1A–S1C). The Syt1 KD reduced the IPSC amplitude elicited by isolated action potentials >90% (Fig. 1A), and similarly suppressed the initial IPSCs elicited by a 10 or 50 Hz action-potential train (Figs. 1B, S1D and S1E). The Syt1 KD phenotype was rescued by expression of wild-type shRNA-resistant Syt1, confirming the specificity of the KD (Fig. 1A). However, as described for the Syt1 knockout (Maximov and Südhof, 2005), the Syt1 KD did not block release induced by stimulus trains. Instead, Syt1 KD neurons exhibited in response to stimulus trains a significant amount of delayed asynchronous release that manifested as a slow form of facilitating synaptic transmission (Figs. 1B, S1D, and S1E). As a result, the Syt1 KD only modestly decreased the total synaptic charge transfer induced by high-frequency stimulus trains, although the time course of the charge transfer was dramatically delayed. In contrast, TetTox completely blocked synaptic transmission in response to isolated action potentials or trains of action potentials (Figs. 1A, 1B, S1D, and S1E).

Thus, the Syt1 KD impairs synaptic transmission induced by isolated action potentials and alters the kinetics but not the overall amount of transmission induced by bursts of actions potentials, effectively resulting in a high-pass filter (Fig. 1C). The slow release that is observed in Syt1 KD neurons (and Syt1 knockout neurons; Maximov and Südhof, 2005) is likely due to a nonphysiological activation of fusion by ancillary Ca^{2+}-sensors that do not normally trigger release to a significant extent, but are unclamped by the loss of Syt1 (Maximov and Südhof, 2005, Sun et al., 2007).

Erasure of synchronous transmission in the hippocampus

We next explored the possibility that the Syt1 KD could be used for manipulating synaptic transmission *in vivo*. We generated recombinant adeno-associated viruses (AAVs) of a new serotype (AAV-DJ; Grimm et al., 2008) to either express only EGFP (control) or only TetTox, or to express both EGFP and the Syt1 shRNA. Two weeks after *in vivo* stereotactic injection of AAV-DJs into the CA1 region and dentate gyrus (DG) of the hippocampus, we observed widespread neuronal infection with extensive EGFP expression throughout the dorsal hippocampus and part of the ventral hippocampus; high-magnification images confirmed that nearly all neurons at CA1 and DG regions were targeted (Fig. 2A). Only a small number of CA3 neurons expressed EGFP. Virus also sparsely infected the adjacent posterior cingulate cortex and a few neurons in the entorhinal cortex, indicating limited diffusion and/or retrograde transport.

We then used electrophysiological recordings in acute brain slices from injected mice to determine whether the Syt1 KD produced the same phenotype in the brain as in cultured neurons (Fig. 2B). Whole-cell recordings in pyramidal neurons of the subiculum (the major output region for hippocampal CA1 neurons) after stimulation of CA1-derived axons in the alveus revealed that the Syt1 KD almost completely ablated EPSCs evoked by isolated action potentials (Figs. 2C and 2D). In blocking synaptic transmission under these conditions, the Syt1 KD was nearly as effective as tetanus toxin, and this block could not be overcome by increasing the stimulation strength. However, similar to what we observed in cultured neurons (Fig. 1), the Syt1 KD did not ablate EPSCs evoked by trains of action potentials, but only dramatically changed the kinetics of these EPSCs (Figs. 2E, 2F, S2A, and S2B). High-frequency stimulus trains activated in Syt1 KD neurons a delayed form of synaptic transmission that manifested as facilitation during the stimulus trains (Figs. 2E and 2F).

To examine whether short spike bursts observed *in vivo* in CA1 pyramidal neurons are capable of triggering asynchronous release in Syt1 KD neurons, we performed a systematic analysis of synaptic transmission induced by 3, 5, and 10 action potentials triggered at frequencies of up to 200 Hz. Previous studies in the dorsal hippocampus of behaving mice

showed that CA1 pyramidal cells are relatively quiet with an overall average spike frequency of only ~1 Hz, but that ~50% of these spikes are part of complex spike bursts composed of 2–6 spikes firing at 50–200 Hz (Harris et al., 2001; Harvey et al., 2009; Jones and Wilson, 2005; Ranck, 1973), which corresponds well with the spike bursts we are examining here. Remarkably, we found that bursts of only 3 spikes elicited significant asynchronous release in Syt1 KD neurons, suggesting that the Syt1 KD introduces a high-pass filter even for short spike bursts (Figs. 2E, 3F, S2A, and S2B). Moreover, long-term potentiation (LTP) could still be elicited in Syt1 KD synapses (Fig. S2C). Parallel experiments confirmed that TetTox completely blocked all transmission induced by isolated or repeated action potentials (Figs. 2C and 2D and data not shown). Thus, the phenotype produced by *in vivo* expression of the Syt1 KD replicates the *in vitro* phenotype, demonstrating that the Syt1 KD similar to TetTox abrogates synaptic transmission induced by isolated spikes, but different from TetTox only alters the kinetics but not the magnitude of synaptic transmission induced by high frequency bursts of spikes.

Effect of the Syt1 KD on local field oscillations in the hippocampus *in vivo*

We next examined the effect of the Syt1 KD on the electrophysiological activities of neurons in awake, freely moving mice. Hippocampal theta oscillations are critical for hippocampus-dependent learning and memory (Buzsaki, 2002; Goutagny et al., 2009). Theta oscillations are generated by a combination of synchronized excitatory inputs to CA1 and of local neuronal activity, especially the activity of local interneurons that may produce feedback inhibition onto medial septum neurons for pacemaking of oscillations (Buzsaki, 2002). Recent studies indicated that theta pacemaking may originate in the CA1 region, providing further support for the hypothesis that CA1-region local neurons are critical for theta oscillation (Goutagny et al., 2009). The AAV infection in our experiments included all CA1 pyramidal cells and interneurons as well as most DG neurons (which influence CA1 region activity via direct innervation of CA3 region neurons), providing us with a system to evaluate the impact of manipulations of synaptic transmission on local oscillations.

We recorded local field potentials in CA1 in awake, freely moving mice, and found that TetTox significantly reduced the power of theta oscillations, consistent with a critical role of the infected neurons in the generation of these oscillations (Figs. 3A–3C). In contrast to TetTox, however, the Syt1 KD did not reduce the overall power of the oscillations, but produced a shift in the peak frequency of the theta oscillations towards slightly higher frequencies (Figs. 3A–3C). These results suggest that the residual synaptic release induced by spike bursts after the Syt1 KD is sufficient for the generation of theta oscillations. It appears likely that the change in synaptic transmission induced by the Syt1 KD altered the interaction between the hippocampus and septum, thereby shifting the peak frequencies. Although it is premature to provide a mechanistic account for this observation since the exact location and mechanism of pacemaking of theta oscillations are not yet clear, these results further demonstrate that the Syt1 KD does not simply block the communication between neurons, but rather institutes a filter that permits selective propagation of high-frequency information. It needs to be noted that a small group of interneurons in the hippocampus express Syt2 instead of Syt1 (Kerr et al., 2008) and would not be affected by the Syt1 KD, and may contribute to the generation of theta oscillations.

Impact of hippocampal Syt1 KD on contextual memory

To examine whether synaptic transmission mediated by isolated spikes and/or precise timing of synaptic transmission triggered by spike bursts in the hippocampus are essential for learning and memory, we tested the effect of the hippocampal Syt1 KD on contextual and cued fear conditioning. We trained mice in a conditioning chamber with three tone/footshock pairs, and examined 'freezing' as evidence of fear memory under three conditions:

when the mice were placed into the same chamber used for training (contextual fear conditioning); when the mice were placed into a similar but altered chamber (altered context, to monitor the precision of memory), and finally when the mice were exposed to the conditioning tone in the altered chamber (cued fear conditioning). Previous studies showed that similar to human declarative memory, contextual fear memory in rodents undergoes a consolidation process. Recent fear memory (i.e., memory in the days following the memorable event) depends on hippocampal function, whereas remote memory (i.e., memory after several weeks) operates independent of hippocampal function (Frankland and Bontempi, 2005; Frankland et al., 2004; Kim and Fanselow, 1992; Squire et al., 2004). Therefore, we carried out our experiments using two protocols. First, to monitor recent memories, we injected AAVs into the hippocampus 30 days BEFORE training, and tested memory 1–2 days after training (Fig. 4A). Second, to monitor remote memories, we injected AAVs into the hippocampus 7–10 days AFTER training, and tested memory 27–30 days after the injection (i.e., ~36 days after training; Fig. 4E).

In tests of recent memory (Figs. 4B–4D), hippocampal TetTox severely impaired contextual memory, consistent with previous studies demonstrating that the hippocampus is critical for contextual fear learning (Fanselow and Dong, 2010; Kim and Fanselow, 1992; Wiltgen et al., 2006). However, the Syt1 KD caused no significant impairment in contextual memory (Fig. 4B). In the altered context test, the hippocampal Syt1 KD produced an increased fear response, suggesting that the Syt1 KD impaired the mouse's ability to recognize the context as different (Fig. 4C), consistent with its electrophysiologically demonstrated effectiveness (Fig. 3). Since TetTox blocks contextual fear conditioning (Fig. 4B), it does not result in an increased fear response in the altered context (Fig. 4C). Furthermore, as expected neither the Syt1 KD nor TetTox produced a significant change in cued fear conditioning (Fig. 4D). No alterations of spontaneous behaviors were observed in the injected mice, as assessed by quantitative actometer measurements (Fig. S3; Fowler et al., 2003 and 2001). The fact that contextual fear memory is normal after the hippocampal Syt1 KD but is blocked by TetTox strongly suggests that CA1 neurons can rely on bulk synaptic transmission induced by bursts of spikes for transmitting information to their downstream targets during fear conditioning learning.

Consistent with previous work suggesting that the hippocampus does not play a major role in remote memories (Fanselow and Dong, 2010; Frankland and Bontempi, 2005; Frankland et al., 2004; Kim and Fanselow, 1992), the hippocampal Syt1 KD or TetTox had no significant effect on remote memory, except for a small impairment of contextual fear conditioning by TetTox (Figs. 4E–4H). This effect of TetTox may reflect a limited role of the hippocampus in the consolidation of memory in the first few weeks after training (Nakashiba et al., 2009).

Impact of entorhinal Syt1 KD on contextual memory

The lack of an effect of the hippocampal Syt1 KD on contextual fear conditioning was surprising, given that synaptic transmission triggered by isolated spikes – accounting for ~50% of hippocampal firing (Jones and Wilson, 2005) – is blocked by the Syt1 KD, and that the Syt1 KD additionally severely delays and broadens the time course of synaptic transmission triggered by bursts of spikes. To assess whether isolated spikes are generally dispensable for neuronal function, we introduced the Syt1 KD into the entorhinal cortex, which is adjacent to the hippocampus and directly and indirectly influences the activity of CA1 pyramidal neurons (Fig. 5A). Expression of TetTox light chain in the entorhinal cortex suppressed all recent memory, including somewhat surprisingly cued fear conditioning (Figs. 5B–5D). The Syt1 KD also significantly impaired contextual fear conditioning, but not cued fear conditioning (Figs. 5B–5D). Thus, synchronous neurotransmission elicited by single spikes is essential for entorhinal function in contextual fear conditioning.

Suppression of synchronous transmission in the medial prefrontal cortex

To further explore whether the limited role of isolated spikes in hippocampal-dependent contextual memory applies to other brain areas, we examined the effect of the Syt1 KD in the medial prefrontal cortex on contextual fear conditioning. The medial prefrontal cortex, commonly considered to be critical for the "executive control" of behaviors, is essential for remote but not recent fear memories. After injection of recombinant AAVs into the prefrontal cortex, EGFP-expressing neurons were present in all major subregions of the mPFC, including the anterior cingulate, the prelimbic, and the infralimbic cortex (Figs. 6A, 6B, and S4). Electrophysiological recordings from pyramidal cells in acute slices revealed that the Syt1 KD produced an impairment in synaptic transmission similar to that observed in the hippocampus. The extent of the impairment in synaptic transmission was less severe, however, presumably because afferent fibers derived from non-infected brain regions innervate the cells from which recordings were made (Figs. 6C–6E).

Impact of the Syt1 KD in the prefrontal cortex on contextual memory

In behavioral tests, neither the Syt1 KD nor TetTox in prefrontal cortex significantly impaired acquisition of recent fear memories. Unexpectedly, however, both treatments increased freezing in response to the altered context, indicating over-generalization of contextual memories (Figs. 7A–7C). Thus, the ability to recognize the precise context of a threatening environment (a form of pattern separation) in recent memory requires the prefrontal cortex, and specifically involves fast synchronous synaptic transmission mediated by the prefrontal cortex.

Since the prefrontal cortex is known to contribute to remote memories, we next examined the effect of the Syt1 KD and of TetTox on long-term fear memories. Both similarly impaired contextual and cued fear conditioning, as well as memory in the altered context (Figs. 7D–7F). Consistent with previous studies (Frankland and Bontempi, 2005; Frankland et al., 2004), the reduced freezing to the training context indicates a critical role for the prefrontal cortex in the storage and/or retrieval of remote memories. The reduced freezing to the tone cue may suggest that remote memory of cued auditory fear-conditioning is also dependent on the medial prefrontal cortex. Alternatively, since the tone test was performed in the altered context which contained cues to the original training context, freezing to the tone may have been confounded by contextual memory. Again, no major impairments of spontaneous behaviors were observed in force-plate actometer analyses after Syt1 KD or TetTox injections into the prefrontal cortex (Fig. S5). The finding that prefrontal Syt1 KD and TetTox in the medial prefrontal cortex produced similar effects on fear learning and memory suggests that fast, synchronous synaptic transmission mediated by isolated spikes is indispensible for maintenance and/or retrieval of long-term memories in this brain structure.

DISCUSSION

Here, we used two distinct molecular manipulations of synaptic transmission to explore the role of the hippocampus and prefrontal cortex in recent and remote contextual memory: 1. Block of all synaptic transmission by TetTox and 2., Modulation of the mode of synaptic transmission using the Syt1 KD which selectively abrogates synaptic transmission induced by isolated spikes. We find that block of synaptic transmission in the hippocampus by TetTox impairs recent but not remote contextual fear memory, whereas block of synaptic transmission in the medial prefrontal cortex abrogated remote but not recent fear memory. These results are consistent with previous findings that the hippocampus has a time-limited role in encoding declarative memory, and that the neocortex is critical for long-term storage of consolidated memory (Fanselow and Dong, 2010; Frankland and Bontempi, 2005; Frankland et al., 2004; Kim and Fanselow, 1992; Squire et al., 2004).

In contrast to TetTox, the Syt1 KD yielded unexpected results, with the most striking finding being that the hippocampal Syt1 KD did not impair acquisition of contextual memory despite the fact that such acquisition was dependent on hippocampal function, as confirmed by the TetTox treatment. The result indicates that isolated spike transmission in the hippocampus is not required for acquisition of contextual fear memory, and that hippocampal neurons can rely solely on bursts of spikes to transfer information during memory encoding. This observation is consistent with a study of hippocampal place cells showing that the spatial locations of rats could be read out by looking only at spike bursts (Harris et al., 2001). In contrast to the hippocampal Syt1 KD, the prefrontal Syt1 KD produced the same behavioral phenotype as TetTox both in recent and in remote memory tests, suggesting that isolated spikes and/or the precise timing of spikes are pivotal to the functions of the prefrontal cortex, and that the hippocampus and prefrontal cortex use different spike coding schemes for information processing, at least with respect to the acquisition and maintenance/retrieval of fear memory.

The finding that the hippocampus can rely solely on bursts of spikes to transfer information to its downstream brain structures provides strong evidence for the hypothesis that bursts of spikes act as units of transmission to increase the reliability of communication between neurons (Izhikevich et al., 2003; Lisman, 1997). The effect of the hippocampal Syt1 KD on the precision of fear memory, i.e. the inability of these mice to recognize an altered context, may be due to the expression of the Syt1 KD in the dentate gyrus, since pattern separation is thought to critically involve synaptic transmission at dentate gyrus to CA3 connections (Clelland et al., 2009; Leutgeb et al., 2007; McHugh et al., 2007; Ruediger et al., 2011). If so, this result would suggest that precisely timed synaptic transmission mediated by granule cells (probably newborn granule cells; see Aimone et al., 2011) is essential for pattern separation. Thus, even within the hippocampus, different neuronal circuits may employ distinct coding schemes by relying on isolated spikes or bursts of spikes for execution of critical functions. These different coding schemes may reflect different strategies to handle the differential need of specific circuits for speed versus capacity in information processing when facing limited information processing resources (Varshney et al., 2006). It should be noted that neuronal computations by brain circuits are complex. For example, excitatory neurons not only directly activate downstream structures, but also initiate feed-forward and feed-back inhibition of themselves and surrounding and downstream excitatory neurons by activating inhibitory interneurons. At present it is unclear how local inhibitory networks contribute to the computation of memory by the hippocampus. However, the Syt1 KD will equally affect excitatory and inhibitory outputs (Maximov and Südhof, 2005), and thus allow feed-forward and feed-back inhibition only during spike burst firing.

The timing of spikes carries important information for brain computation. As an example, hippocampal place cells change their timing of firing relative to the phase of the theta oscillation of local field potentials depending on the spatial location of the animal. This “phase precession” is proposed to act as a “temporal code” in the hippocampus, in addition to “rate coding” which is manifested by the firing rate (Ahmed and Mehta, 2009; Harvey et al., 2009). Similarly, studies on spike-timing dependent plasticity (STDP) indicated that a slight alteration in the relative timing of spikes between connected neurons may produce opposite effects on the direction of synaptic plasticity (Dan and Poo, 2006; Nevian and Sakmann, 2006). Despite these observations and numerous theoretical considerations, however, it is difficult to directly test the importance of spike timing in behaving animals due to the lack of approaches to control spike timing. The fact that neurons depend on synaptic transmission to propagate information encoded in spikes to downstream neurons makes it possible to gain insights into the these questions by manipulating synaptic transmission. The Syt1 KD delivered by AAVs described here provided a tool to study the role of synaptic transmission triggered by isolated spikes vs. bursts of spikes, especially

combined with parallel TetTox experiments, and may also be useful for studying other behavioral tasks or brain regions.

The observation that the prefrontal TetTox expression or Syt1 KD impaired the precision of recent fear memory was surprising, suggesting that besides the hippocampus (Frankland et al., 1998; Ruediger et al., 2011), the medial prefrontal cortex is critically involved in determining the precision of contextual memory. Over-generalization of fear memories is critically involved in the development of anxiety disorders such as post-traumatic stress disorder (PTSD) and panic disorders. In addition, patients with these disorders normally show aberrant functions in the medial prefrontal cortex (Britton et al., 2011). It will be interesting to further dissect the neuronal circuits and molecular mechanisms involved in this phenomenon, using approaches outlined here, to determine whether over-generalization of fear memories does indeed involve the medial prefrontal cortex.

The memory function of the prefrontal cortex is consistent with its role as a high-level multimodal association region, but similar to previous studies, our data do not distinguish between a role in retrieval, storage of remote memory, or both (Rudy et al., 2005). The AAV-DJ-mediated local manipulations of gene expression provide an efficient and convenient way for functional dissection of the prefrontal cortex. Further improvements in the techniques, such as inducible and reversible manipulations (Mayford et al., 1996) in combination with *in vivo* imaging (Hubener and Bonhoeffer, 2010) may shed more light on these issues.

Experimental Procedures

Vector construction

Four lentiviral vectors were constructed. Control vector contains a H1 promoter followed by a U6 promoter and an ubiquitin promoter driving mcherry expression. To construct Syt1 KD vector, short hairpin sequence containing syt1 sequence 5'- gag caa atc cag aaa gtg caa -3' was cloned into Xho1-Xba1 locus downstream of the H1 promoter of control vector. In TetTox vector, tetanus toxin light chain (GenBank: L19522.1) was cloned into EcoR1 locus downstream of the ubiquitin promoter of FUW vector. Syt1 KD + rescue vector was constructed by changing mCherry in Syt1 KD vector to EGFP and shRNA-resistant syt1 gene linked in frame by 2A sequences derived from foot-and-mouth disease virus (Okita et al., 2008). ShRNA-resistant syt1 was made by mutating syt1 sequence 5'- gag caa atc cag aaa gtg caa -3' into 5'- gaa cag att caa aag gtc caa -3'. Three AAV vectors were constructed. In control vector, the following components were arranged sequentially downstream of left-ITR of AAV2: CMV promoter and beta-globin intron, EGFP, hGH poly A sequence, H1 promoter, SV40 poly A sequence and right ITR. In Syt1 KD AAV vector, syt1 short hairpin sequence was cloned into the Xho1-Xba1 locus downstream of H1 promoter of control vector. In TetTox vector, the following components were arranged sequentially downstream of the left-ITR: CMV promoter and beta-globin intron, EGFP and TetTox linked in frame by 2A sequence as described above, hGH poly A and the right ITR.

Lentivirus packaging, infection and recording of cultured neurons

Lentivirus and cortical culture were prepared and recorded as described (Maximov et al., 2007; Pang et al., 2010). Neurons derived from P0 (postnatal day 0) or P1 mice were infected with lentivirus at 5–6 DIV (days in vitro) and recorded at 15–16 DIV. Cultured neurons were transferred to extracellular solution containing (in mM; at room temperature with pH 7.4) 140 NaCl, 5 KCl, 2 $CaCl_2$, 2 $MgCl_2$, 10 HEPES and 10 glucose. The neurons were patched with pipettes with resistance between 3 and 4 MΩ and clamped at −70 mV. The patch pipette was filled with intracellular solution containing the following components

(in mM; at room temperature with pH 7.4): 135 CsCl, 10 HEPES, 1 EGTA, 1 Na-GTP, 4 Mg-ATP, and 10 QX-314 [*N*-(2,6-dimethylphenylcarbamoylmethyl) triethylammonium bromide]. Synaptic current was evoked by 90 μA/1 ms current injections via concentric bipolar electrode (CBAEC75, FHC) placed ~150 μm to the patched neurons. IPSCs was isolated by adding AMPA and NMDA receptor blockers CNQX (20 μM) and AP-5 (50 μM) in the extracellular solution. The frequency, duration, and magnitude of the extracellular stimulus were controlled with a model 2100 Isolated Pulse Stimulator (A-M Systems) synchronized with Clampex 10.2 data acquisition software (Molecular Devices). Synaptic currents were monitored with a Multiclamp 700B amplifier (Molecular Devices). Synaptic currents were sampled at 10 kHz and analyzed offline using Clampfit 10.2 (Molecular Devices) software. For graphic representation, the stimulus artifacts of the current traces were removed.

AAV preparation

AAVs were packaged with AAV-DJ capsids for high efficiency *in vivo* neuronal infection. Virus was prepared with a procedure as described (Zolotukhin et al., 1999). Briefly, AAV vectors were co-transfected with pHelper and pRC-DJ into AAV-293 cells. 72 hr later, cells were collected, lysed and loaded onto iodixanol gradient for centrifugation at 400,000g for 2 hrs. The fraction with 40% iodixanol of the gradient was collected, washed and concentrated with 100,000 MWCO tube filter. The infectious titer of virus was measured by infecting HEK293 cells. The concentrations of virus used for stereotaxic injection were adjusted to 1.0×10^7 infectious units/μl (except that for TetTox AAV, for which the highest titer obtained, 8.8×10^6, was used).

Stereotaxic injection

C57BL/6 mice were anesthetized with tribromoethanol (125–250 mg/kg). Viral solution was injected with a glass pipette at a flow rate of 0.15 μl/min. Coordinates used for the hippocampal injection were AP +1.95 mm, ML ±1.25 mm, DV −1.20 mm (for CA1) and −1.95 mm (for DG). 1 μl of viral solution was injected in CA1 and another 1 μl in DG. The coordinates used for the prefrontal injection were AP −1.0 mm, ML ±0.3 mm, DV−1.0 mm and −1.5 mm. The sites at DV−1.0 mm and −1.5 mm both received 1 μl of injection. The coordinates used for the entorhinal injection were AP +4.5 mm, ML ±3.5 mm, DV−4.0 mm. The injections were bilateral except otherwise noted.

Slice Electrophysiology

2-month old C57BL/6 mice were injected with AAVs and were used for slice physiology 3–4 weeks after the infection. Transverse hippocampal slices or coronal prefrontal slices (250 μm) were cut in ice cold solution comprising (in mM): 75 Sucrose, 75 NaCl, 2.5 KCl, 1 NaH2PO4, 8 MgSO4, 0.5 CaCl2, 26.2 NaHCO3, 20 D-glucose saturated with 95% O2/ 5% CO2 and transferred to a holding chamber containing artificial cerebrospinal fluid (ACSF) composed of (in mM): 117.5 NaCl, 2.5 KCl, 1 NaH2PO4, 1.3 MgSO4, 2.5 CaCl2, 26.2 NaHCO3, 11 D-glucose to recover for at least one hour at room temperature before being transferred to a recording chamber continually perfused (1 ml/min) with oxygenated ACSF (maintained at 27–29° C) containing 50 μM of picrotoxin. Whole-cell voltage-clamp recordings were made with 3–5 MΩ pipettes filled with internal solution containing (in mM): 135 CsMeSO4, 10 HEPES, 8 NaCl, 0.25 EGTA, 2 MgCl2, 4 Mg ATP, 0.3 NaGTP and 5 Phosphocreatine (pH 7.3). Neurons were clamped at −65 mV for recording of EPSC in hippocampal slices. In the prefrontal slices neurons were clamped at +30 mV to record NMDAR-mediated EPSCs in the presence of 10 μM of NBQX.

Local Field Recording

2-month old mice were injected with AAVs and were implanted with recording electrodes 2–3 weeks later. Field potential recordings were obtained from the CA1 field of the right, dorsal hippocampus. To implant electrodes, mice were sedated with diazepam (10 mg/kg, i.p.), anesthetized with isoflurane (1–3%), placed in a stereotaxic frame, maintained on a heating pad, and prepared for aseptic surgery. A hole was drilled 2.2 mm posterior and 1.6 mm right of bregma. An insulated, 50 μm diameter stainless steel wire (California Fine Wire) was implanted 1.7 mm below the surface of the brain. The reference electrode was placed in the cerebellum. Two screws were placed in the skull. Electrode leads were connected to pins that were inserted into a strip connector, which was attached to the screws and skull with cranioplastic cement. Following surgery, mice were kept warm and received lactated ringer's with dextrose, antibiotic (enrofloxacin, 10 mg/kg, s.c.), and analgesic (buprenorphine, 0.05 mg/kg, s.c.). After recovering for 7 d, mice were monitored for at least 6 h by EEG recording and simultaneous videotaping. Recordings were obtained with epoch transmitter and receiver tray for wireless EEG (Ripple LLC) and a Cyberamp 380 (Molecular Devices). Signals were amplified, filtered (1–100 Hz), and sampled at 200 Hz (PClamp, Molecular Devices). The whole 6-hr recording was divided into 5-min sessions. Based on the behavioral states of the mice, each session was classified as "exploration", "motionlessness" or a situation which cannot be categorized into these two situations with the following criteria: if a mouse was exploring the recording chamber for more than 3 minutes in a 5-min session, this session will be classified as "exploration"; if a mouse was immobile (no apparent movement except breathing and slight shaking of head or body) for more than 4 minutes in a 5-min session, this session will be classified as "motionlessness". The power spectrums of each 5-min session were generated and the power spectrums from the same behavioral category were averaged together with Clampfit10.2 (Axon Laboratory). The wavelet spectrums of representative traces were produced by AutoSignal1.7.

Fear Conditioning

2 month-old male C57BL/6 mice (Charles River) were housed individually with normal 12/12 hr daylight cycle. They were handled daily for 5 days prior to training. On training day, mice were placed in fear conditioning chamber (H10–11M-TC, Coulbourn Instruments, PA) located in the center of a sound attenuating cubicle (Coulbourn Instruments). The conditioning chamber was cleaned with 10% ethanol to provide a background odor. A ventilation fan provided a background noise at ~55 dB. After a 2 min exploration period, 3 tone-footshock pairings separated by 1 min intervals were delivered. The 85 dB 2 kHz tone lasted for 30 s and the footshocks were 0.75 mA and lasted for 2 s. The foot shocks co-terminated with the tone. The mice remained in training chamber for another 30 seconds before being returned to home cages. In context test, mice were placed back into the original conditioning chamber for 5 min. The altered context and tone tests were conducted in a new room. The same conditioning chamber were moved to this room and modified by changing its metal grid floor to a plastic sheet, white metal side walls to plastic walls decorated with red stripes, background odor of ethanol to vanilla. The ventilation fan was turned off to reduce background noise. Mice were placed in the altered chamber for 5 min to measure the freeze level in the altered context and after this 5-min period a tone (85 dB, 2 kHz) was delivered for 1 min to measure the freeze to tone. The behavior of the mice was recorded with the Freezeframe software and analyzed with Freezeview software (Coulbourn Instruments). Motionless bouts lasting more than 1 second were considered as freeze. Animal experiments were conducted following protocols approved by Administrative Panel on Laboratory Animal Care at Stanford University.

Histochemistry

Mice were anesthetized with tribromoethanol and perfused with 10 ml of PBS followed by 50 ml of fixative (4% paraformaldehyde diluted in PBS). The brains were removed and post-fixed for 3 hours at room temperature and then immersed in 30% sucrose solution overnight before being sectioned at 30 μm-thickness on a cryostat. The free-floating brain sections were collected in PBS and counterstained with DAPI. The brain sections were mounted onto glass slides with Vectashield mounting medium (Vector Laboratories, CA). Micoscopic photos were taken with a Leica DM IRE2 microscope. Photos taken with 10X objective were tiled to generate the image of the whole brain sections.

Immunoblotting

Cultured neurons were homogenized in lysis buffer (1% SDS, 10 mM Tris), mixed with 6× loading buffer (0.5 M tris, 60% glycerol, 10% SDS, 10% Beta-Mercaptoethanol and 0.01% bromphenol blue) and denatured at 100°C for 20 min. After centrifugation at 14,000 rpm for 30 min the supernatants were loaded for SDS-PAGE and immunoblotted with standard chemiluminescence protocols. The primary antibodies used in the study include: anti-syt1 (CL41.1), anti-syb2 (CL69.1) and Synx1 (U6251). Blots were digitized and quantified with NIH image software. All band intensities were normalized to that of control samples.

Highlights

- Burst-evoked synaptic transmission suffices to entrain hippocampus-dependent memory
- Precisely timed spikes are indispensible for prefrontal cortex-dependent memory
- Prefrontal cortex and hippocampus determine the precision of contextual memories
- AAV DJ allows efficient brain region-specific manipulation of gene expression

Supplementary Material

Refer to Web version on PubMed Central for supplementary material.

Acknowledgments

We thank Drs. Mark Kay (Stanford University) and Eric J. Nestler (Mount Sinai Medical School NY) for AAV vectors and AAV preparation protocols.

REFERENCES

Ahmed OJ, Mehta MR. The hippocampal rate code: anatomy, physiology and theory. Trends Neurosci. 2009; 32:329–338. [PubMed: 19406485]

Aimone JB, Deng W, Gage FH. Resolving new memories: a critical look at the dentate gyrus, adult neurogenesis, and pattern separation. Neuron. 2011; 70(4):589–596. [PubMed: 21609818]

Borst JG. The low synaptic release probability in vivo. Trends Neurosci. 2010; 33:259–266. [PubMed: 20371122]

Branco T, Staras K. The probability of neurotransmitter release: variability and feedback control at single synapses. Nat Rev Neurosci. 2009; 10:373–383. [PubMed: 19377502]

Britton JC, Lissek S, Grillon C, Norcross MA, Pine DS. Development of anxiety: the role of threat appraisal and fear learning. Depress Anxiety. 2011; 28:5–17. [PubMed: 20734364]

Burgos-Robles A, Vidal-Gonzalez I, Santini E, Quirk GJ. Consolidation of fear extinction requires NMDA receptor-dependent bursting in the ventromedial prefrontal cortex. Neuron. 2007; 53:871–880. [PubMed: 17359921]

Buzsaki G. Theta oscillations in the hippocampus. Neuron. 2002; 33:325–340. [PubMed: 11832222]

Clelland CD, Choi M, Romberg C, Clemenson GD Jr, Fragniere A, Tyers P, Jessberger S, Saksida LM, Barker RA, Gage FH, et al. A functional role for adult hippocampal neurogenesis in spatial pattern separation. Science. 2009; 325:210–213. [PubMed: 19590004]

Dan Y, Poo MM. Spike timing-dependent plasticity: from synapse to perception. Physiol Rev. 2006; 86:1033–1048. [PubMed: 16816145]

Fanselow MS, Dong HW. Are the dorsal and ventral hippocampus functionally distinct structures? Neuron. 2010; 65:7–19. [PubMed: 20152109]

Fowler SC, Birkestrand B, Chen R, Vorontsova E, Zarcone T. Behavioral sensitization to amphetamine in rats: changes in the rhythm of head movements during focused stereotypies. Psychopharmacology (Berl). 2003; 170:167–177. [PubMed: 12827349]

Fowler SC, Birkestrand BR, Chen R, Moss SJ, Vorontsova E, Wang G, Zarcone TJ. A force-plate actometer for quantitating rodent behaviors: illustrative data on locomotion, rotation, spatial patterning, stereotypies, and tremor. J Neurosci Methods. 2001; 107:107–124. [PubMed: 11389948]

Frankland PW, Bontempi B. The organization of recent and remote memories. Nat Rev Neurosci. 2005; 6:119–130. [PubMed: 15685217]

Frankland PW, Bontempi B, Talton LE, Kaczmarek L, Silva AJ. The involvement of the anterior cingulate cortex in remote contextual fear memory. Science. 2004; 304:881–883. [PubMed: 15131309]

Frankland PW, Cestari V, Filipkowski RK, McDonald RJ, Silva AJ. The dorsal hippocampus is essential for context discrimination but not for contextual conditioning. Behav Neurosci. 1998; 112:863–874. [PubMed: 9733192]

Geppert M, Goda Y, Hammer RE, Li C, Rosahl TW, Stevens CF, Sudhof TC. Synaptotagmin I: a major Ca2+ sensor for transmitter release at a central synapse. Cell. 1994; 79:717–727. [PubMed: 7954835]

Goda Y, Stevens CF. Two components of transmitter release at a central synapse. Proc Natl Acad Sci U S A. 1994; 91:12942–12946. [PubMed: 7809151]

Goutagny R, Jackson J, Williams S. Self-generated theta oscillations in the hippocampus. Nat Neurosci. 2009; 12:1491–1493. [PubMed: 19881503]

Grimm D, Lee JS, Wang L, Desai T, Akache B, Storm TA, Kay MA. In vitro and in vivo gene therapy vector evolution via multispecies interbreeding and retargeting of adeno-associated viruses. J Virol. 2008; 82:5887–5911. [PubMed: 18400866]

Harris KD, Hirase H, Leinekugel X, Henze DA, Buzsaki G. Temporal interaction between single spikes and complex spike bursts in hippocampal pyramidal cells. Neuron. 2001; 32:141–149. [PubMed: 11604145]

Harvey CD, Collman F, Dombeck DA, Tank DW. Intracellular dynamics of hippocampal place cells during virtual navigation. Nature. 2009; 461:941–946. [PubMed: 19829374]

Hubener M, Bonhoeffer T. Searching for Engrams. Neuron. 2010; 67:363–371. [PubMed: 20696375]

Izhikevich EM, Desai NS, Walcott EC, Hoppensteadt FC. Bursts as a unit of neural information: selective communication via resonance. Trends Neurosci. 2003; 26:161–167. [PubMed: 12591219]

Jackson ME, Homayoun H, Moghaddam B. NMDA receptor hypofunction produces concomitant firing rate potentiation and burst activity reduction in the prefrontal cortex. Proc Natl Acad Sci U S A. 2004; 101:8467–8472. [PubMed: 15159546]

Jones MW, Wilson MA. Theta rhythms coordinate hippocampal-prefrontal interactions in a spatial memory task. PLoS Biol. 2005; 3:e402. [PubMed: 16279838]

Kerr AM, Reisinger E, Jonas P. Differential dependence of phasic transmitter release on synaptotagmin 1 at GABAergic and glutamatergic hippocampal synapses. Proc Natl Acad Sci U S A. 2008; 105:15581–15586. [PubMed: 18832148]

Kim JJ, Fanselow MS. Modality-specific retrograde amnesia of fear. Science. 1992; 256:675–677. [PubMed: 1585183]

Leutgeb JK, Leutgeb S, Moser MB, Moser EI. Pattern separation in the dentate gyrus and CA3 of the hippocampus. Science. 2007; 315:961–966. [PubMed: 17303747]

Lisman JE. Bursts as a unit of neural information: making unreliable synapses reliable. Trends Neurosci. 1997; 20:38–43. [PubMed: 9004418]

Maximov A, Pang ZP, Tervo DG, Sudhof TC. Monitoring synaptic transmission in primary neuronal cultures using local extracellular stimulation. J Neurosci Methods. 2007; 161:75–87. [PubMed: 17118459]

Maximov A, Sudhof TC. Autonomous function of synaptotagmin 1 in triggering synchronous release independent of asynchronous release. Neuron. 2005; 48:547–554. [PubMed: 16301172]

Mayford M, Bach ME, Huang YY, Wang L, Hawkins RD, Kandel ER. Control of memory formation through regulated expression of a CaMKII transgene. Science. 1996; 274:1678–1683. [PubMed: 8939850]

McHugh TJ, Jones MW, Quinn JJ, Balthasar N, Coppari R, Elmquist JK, Lowell BB, Fanselow MS, Wilson MA, Tonegawa S. Dentate gyrus NMDA receptors mediate rapid pattern separation in the hippocampal network. Science. 2007; 317:94–99. [PubMed: 17556551]

Meyer AC, Neher E, Schneggenburger R. Estimation of quantal size and number of functional active zones at the calyx of held synapse by nonstationary EPSC variance analysis. J Neurosci. 2001; 21:7889–7900. [PubMed: 11588162]

Nakashiba T, Buhl DL, McHugh TJ, Tonegawa S. Hippocampal CA3 output is crucial for ripple-associated reactivation and consolidation of memory. Neuron. 2009; 62:781–787. [PubMed: 19555647]

Nevian T, Sakmann B. Spine Ca^{2+} signaling in spike-timing-dependent plasticity. J. Neurosci. 2006; 26:11001–11013. [PubMed: 17065442]

Okita K, Nakagawa M, Hyenjong H, Ichisaka T, Yamanaka S. Generation of mouse induced pluripotent stem cells without viral vectors. Science. 2008; 322:949–953. [PubMed: 18845712]

Pang ZP, Cao P, Xu W, Sudhof TC. Calmodulin controls synaptic strength via presynaptic activation of calmodulin kinase II. J Neurosci. 2010; 30:4132–4142. [PubMed: 20237283]

Polsky A, Mel B, Schiller J. Encoding and decoding bursts by NMDA spikes in basal dendrites of layer 5 pyramidal neurons. J Neurosci. 2009; 29:11891–11903. [PubMed: 19776275]

Quinn JJ, Wied HM, Ma QD, Tinsley MR, Fanselow MS. Dorsal hippocampus involvement in delay fear conditioning depends upon the strength of the tone-footshock association. Hippocampus. 2008; 18:640–654. [PubMed: 18306286]

Ranck JB Jr. Studies on single neurons in dorsal hippocampal formation and septum in unrestrained rats. I. Behavioral correlates and firing repertoires. Exp Neurol. 1973; 41:461–531. [PubMed: 4355646]

Rudy JW, Biedenkapp JC, O'Reilly RC. Prefrontal cortex and the organization of recent and remote memories: an alternative view. Learn Mem. 2005; 12:445–446. [PubMed: 16166399]

Ruediger S, Vittori C, Bednarek E, Genoud C, Strata P, Sacchetti B, Caroni P. Learning-related feedforward inhibitory connectivity growth required for memory precision. Nature. 2011; 473:514–518. [PubMed: 21532590]

Sheffield ME, Best TK, Mensh BD, Kath WL, Spruston N. Slow integration leads to persistent action potential firing in distal axons of coupled interneurons. Nat Neurosci. 2011; 14:200–207. [PubMed: 21150916]

Silver RA, Momiyama A, Cull-Candy SG. Locus of frequency-dependent depression identified with multiple-probability fluctuation analysis at rat climbing fibre-Purkinje cell synapses. J Physiol. 1998; 510(Pt 3):881–902. [PubMed: 9660900]

Squire LR, Stark CE, Clark RE. The medial temporal lobe. Annu Rev Neurosci. 2004; 27:279–306. [PubMed: 15217334]

Sun J, Pang ZP, Qin D, Fahim AT, Adachi R, Sudhof TC. A dual-Ca2+-sensor model for neurotransmitter release in a central synapse. Nature. 2007; 450:676–682. [PubMed: 18046404]

Varshney LR, Sjostrom PJ, Chklovskii DB. Optimal information storage in noisy synapses under resource constraints. Neuron. 2006; 52:409–423. [PubMed: 17088208]

Walker AG, Miller BR, Fritsch JN, Barton SJ, Rebec GV. Altered information processing in the prefrontal cortex of Huntington's disease mouse models. J Neurosci. 2008; 28:8973–8982. [PubMed: 18768691]

Wiltgen BJ, Sanders MJ, Anagnostaras SG, Sage JR, Fanselow MS. Context fear learning in the absence of the hippocampus. J Neurosci. 2006; 26:5484–5491. [PubMed: 16707800]

Zhang WN, Bast T, Feldon J. The ventral hippocampus and fear conditioning in rats: different anterograde amnesias of fear after infusion of N-methyl-D-aspartate or its noncompetitive antagonist MK-801 into the ventral hippocampus. Behav Brain Res. 2001; 126:159–174. [PubMed: 11704261]

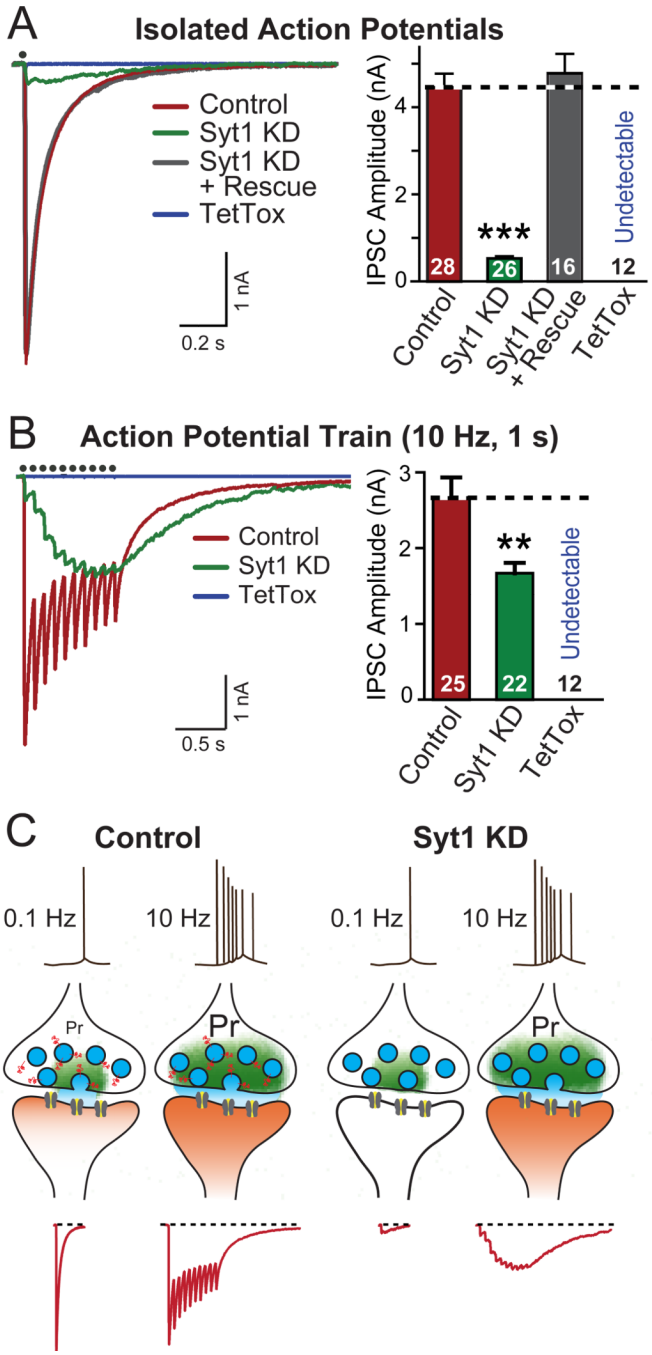

Figure 1. Syt1 KD Effectively Produces a High-pass Frequency Filter for Synaptic Transmission

(**A**) Representative traces (left) and summary graphs of amplitudes (right) of IPSCs recorded in cultured neurons infected with lentiviruses expressing mCherry alone (Control), or together with the Syt1 shRNA (Syt1 KD), Syt1 shRNA and Syt1 rescue protein (Syt1 KD + Rescue), or tetanus toxin ligh chain (TetTox). IPSCs were evoked by single-pulse stimuli, and recorded in whole-cell mode (red: control; green: Syt1 KD; gray: Syt1 KD + Rescue; blue: TetTox). Black dots on top of the traces indicate the time when stimulation was delivered.

(**B**) Same as above, except that IPSCs were evoked by stimulus trains consisting 10 pulses at 10 Hz, and that the summary graphs depict charge transfers during the trains.
(**C**) Schematic illustration of the synaptic effect of the Syt1 KD. Individual isolated spikes propagate to terminals and trigger Ca^{2+}-dependent neurotransmitter release which is mediated by Syt1 as the Ca^{2+}-sensor. The release probability (Pr) of typical forebrain synapses in response to an individual spike is low. Bursts of spikes increase the overall probability of release by leading to an accumulation of Ca^{2+}, and thereby enhance the reliability of transmission. In Syt1 KD neurons, individual spike-triggered synchronous synaptic release — the majority of synaptic release — is blocked, but the accumulating Ca^{2+} stimulates unphysiological delayed release that is asynchronous and during longer stimulus trains produces the same overall synaptic transmission as synchronous release, although with a completely different kinetics.
Data in A and B are means ± SEMs; numbers inside columns indicate the number of neurons analyzed in at least three independent experiments. Statistical significance was calculated by Student's t-test (2-tailed), * $p<0.05$; ** $p<0.01$; *** $p<0.001$. For KD quantitation and additional high-frequency stimulation data, see Fig. S1.

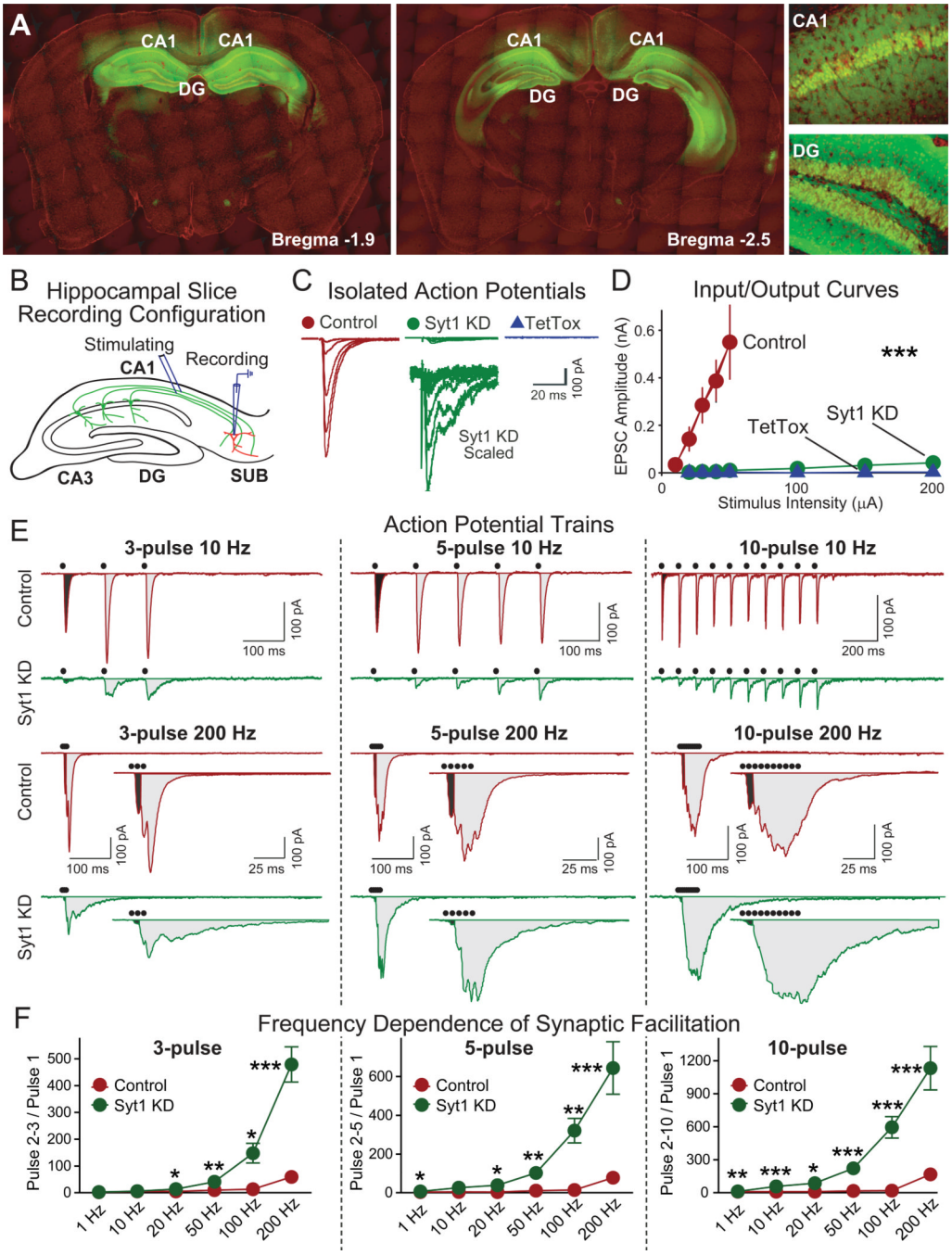

Figure 2. Hippocampal Syt1 KD Erases Synchronous Synaptic Transmission

(**A**) Visualization of EGFP expression after stereotactic injection of EGFP-expressing AAVs into the CA1 and dentate gyrus (DG) regions of the dorsal hippocampus. Two coronal brain sections from the same mouse at different anterior-posterior positions are shown (green, EGFP; red, DAPI counterstain). Recombinant AAV-DJ viruses expressing EGFP were injected into the dorsal hippocampus of 2-month old mice, and EGFP expression was imaged 3 weeks later (CA1, CA1 region; DG, dentate gyrus).

(**B**) Schematic drawing of the electrophysiological recording configuration used to analyze synapses formed by CA1 neurons onto subiculum neurons (SUB). CA1 axons were

stimulated in the alveus, and whole-cell recordings were obtained from pyramidal neurons of the subiculum.

(**C**, **D**) Representative traces (C) and summary graphs of amplitudes (D) of EPSCs elicited by isolated stimuli with increasing stimulation strength (control n=6, Syt1 KD n=12, TetTox n=9).

(**E**, **F**) Representative traces (E) and summary graphs (F) of EPSCs evoked by stimulation trains consisting of 3, 5 or 10 pulses applied at frequencies ranging from 1–200 Hz. The black dots on top of the traces indicate stimulation time points. For the 200 Hz stimulus trains, the entire stimulus train traces are shown on top and the expanded traces of the initial time period are shown on the bottom. In F, facilitation was quantified as the ratio of the charge transfers produced by pulses 2–3, 2–5, or 2–10, respectively, to pulse 1 (for each group, n=5–18).

Data are means ± SEM; Statistical significance between means was determined using Student's t-test (* $p<0.05$, ** $p<0.01$; *** $p<0.001$). Measurements of long term potentiation (LTP) are shown in Figure S2.

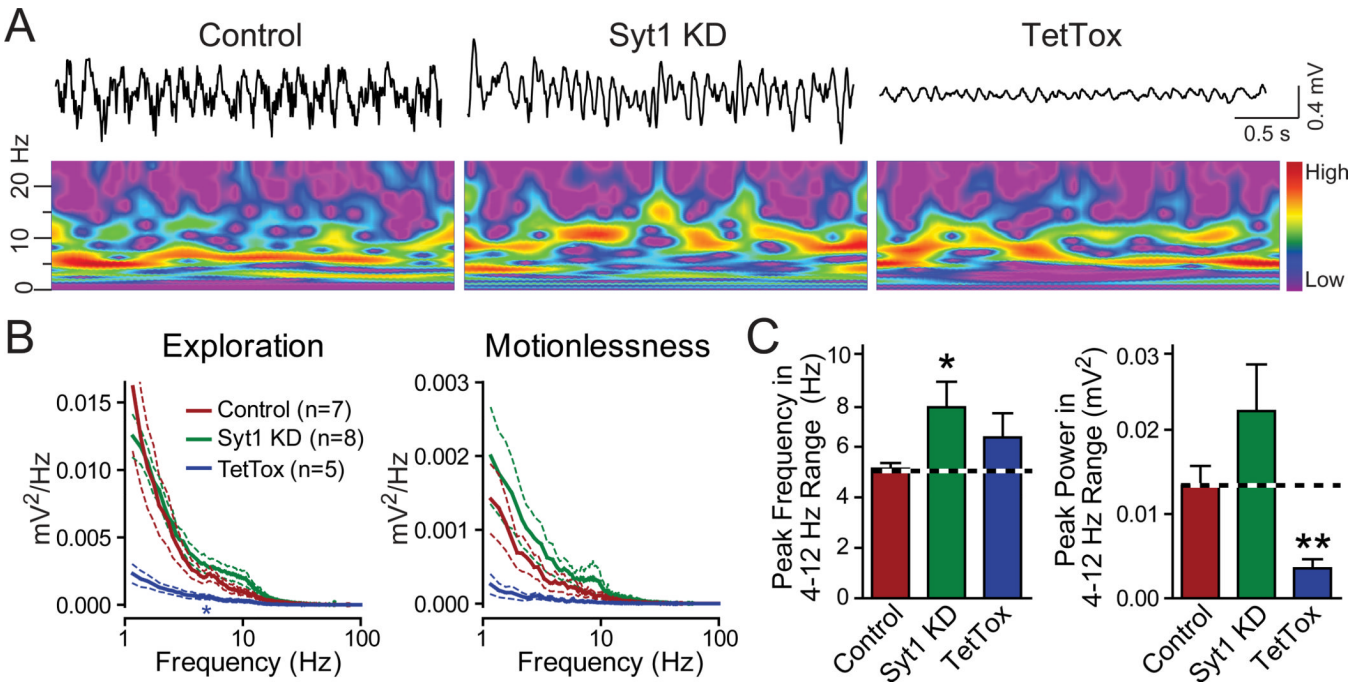

Figure 3. ***In vivo*** **recordings of CA1 local field potentials in freely moving mice**

(**A**) Representative traces and wavelet spectra of CA1 local field potential recordings from mice receiving hippocampal injections of control, Syt1 KD or TetTox AAV, respectively. The colors of the wavelet spectrums are linearly scaled to the level of the power with red representing high power and purple indicating low power.

(**B**) Averaged power spectra of CA1 local field recordings during different behavioral states. Data are means ± SEM; statistical significance between the means of power spectra in the 4–10 Hz range was determined by the repeated measures two-way ANOVA test (* $p<0.05$).

(**C**) Quantitation of the peak frequency in the power spectrum in the theta range (4–12 Hz) and the power at the peak frequency. Data are means ± SEM; statistical significance between means was determined with Student's t-test (* $p<0.05$, ** $p<0.01$).

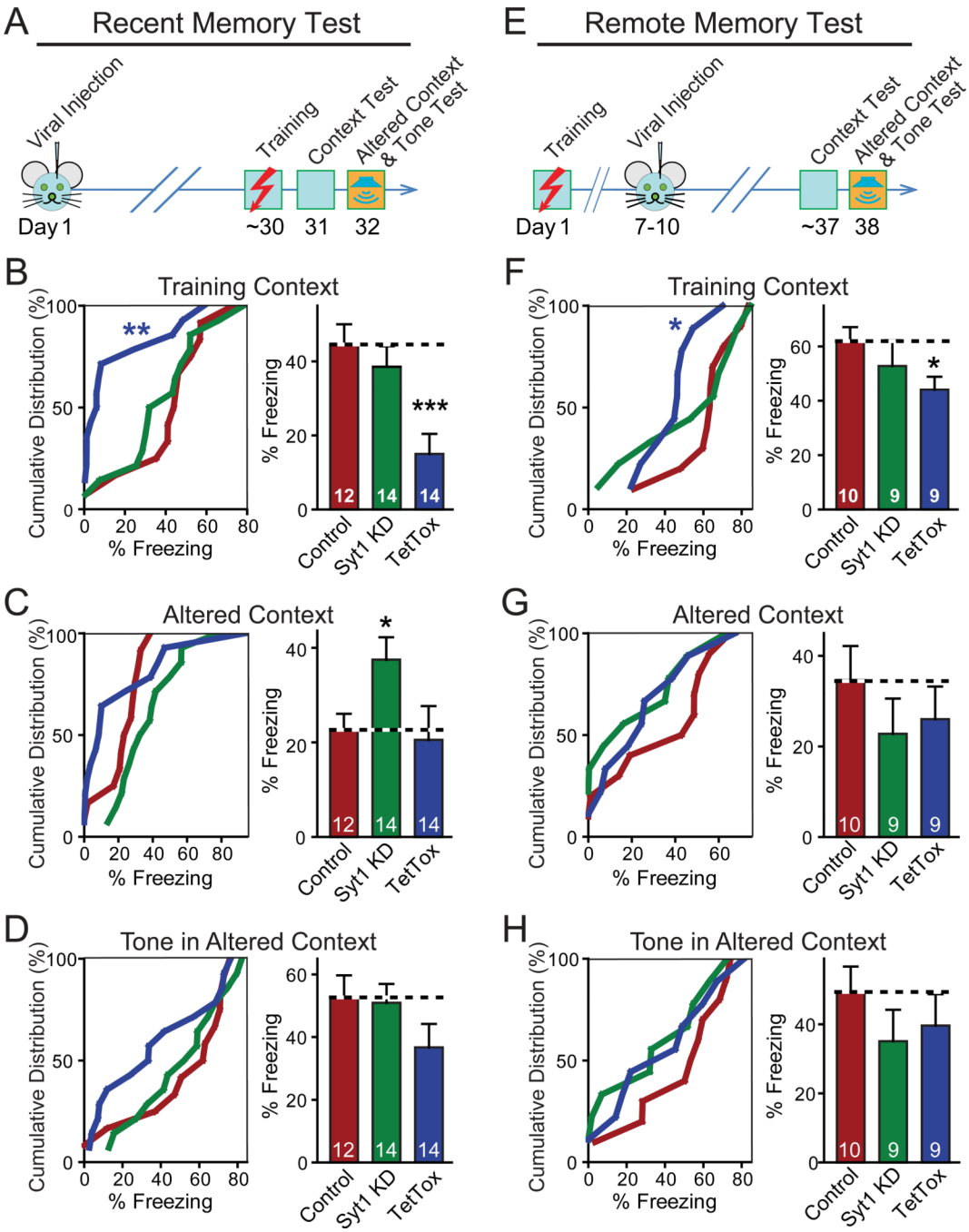

Figure 4. Contextual Memory Persists after Syt1 KD in Hippocampus

(**A**) Design of experiments measuring recent fear memories. Note that fear conditioning was conducted as training context test to measure contextual memory, altered context test (similar cage, but changes in odor, cage floor, wall cues and background noise, etc.) to test the precision of memory, and tone test to measure memory of auditory cues.

(**B–D**) Cumulative distribution (left) and bar graphs (right) of recent fear conditioning memory (measured as freezing) as a function of hippocampal injections of AAVs expressing the Syt1 KD or tetanus-toxin light chain (TetTox).

(**E**) Design of experiments measuring remote fear memories. Note that the measurements of fear conditioning are identical to (A), but that the stereotactic viral injections occur after training.

(**F–H**) Same as B–D, except that the experimental design measures remote memories. Data in bar graphs are means ± SEMs; numbers inside bars indicate the number of mice analyzed. Statistical significance between cumulative distributions was calculated by the Kolmogorov–Smirnov test (two-sample), and between groups (comparing Syt1 KD or TetTox to control) Student's t test (2-tailed); * $p<0.05$; *** $p<0.001$. For analysis of basic behavioral and motor parameters, see Figure S3.

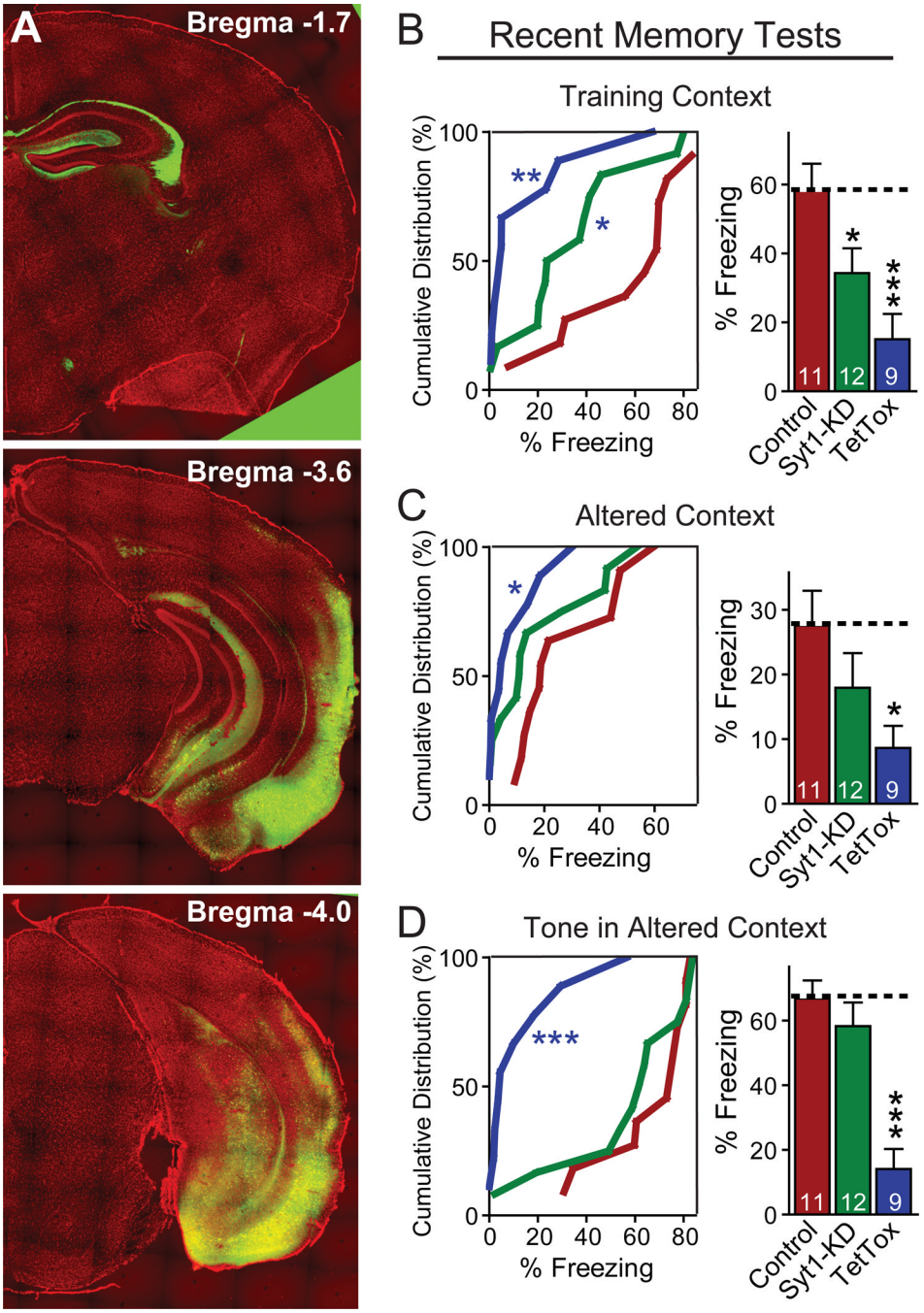

Figure 5. Syt1 KD in the entorhinal cortex modestly impairs recent memories

(**A**) Pattern of EGFP expression after AAV injection into the entorhinal cortex. Three coronal brain sections from the same mouse at different anterior-posterior positions are shown (green, EGFP; red, DAPI counterstain). Neurons in both medial and lateral entorhinal cortex were infected. Virus spread to the adjacent ventral subiculum and ventral hippocampus, with sparse infection of the cortical amygdalar area. Axonal fibers originating from the entorhinal cortex and terminating at the stratum lacunosum-moleculare of the hippocampus are apparent by expression of EGFP.

(**B–D**) Cumulative distribution (left) and bar graphs (right) of recent fear conditioning memory (measured as freezing) as a function of entorhinal injections of AAVs expressing the Syt1 KD or tetanus-toxin light chain (TetTox). The experimental procedure was the same as that described in Fig4A. Data in bar graphs are means ± SEMs; numbers inside bars indicate the number of mice analyzed. Statistical significance between cumulative distributions was calculated by the Kolmogorov–Smirnov test (two-sample), and between groups (comparing Syt1 KD or TetTox to control) Student's t test (2-tailed); * $p<0.05$; *** $p<0.001$.

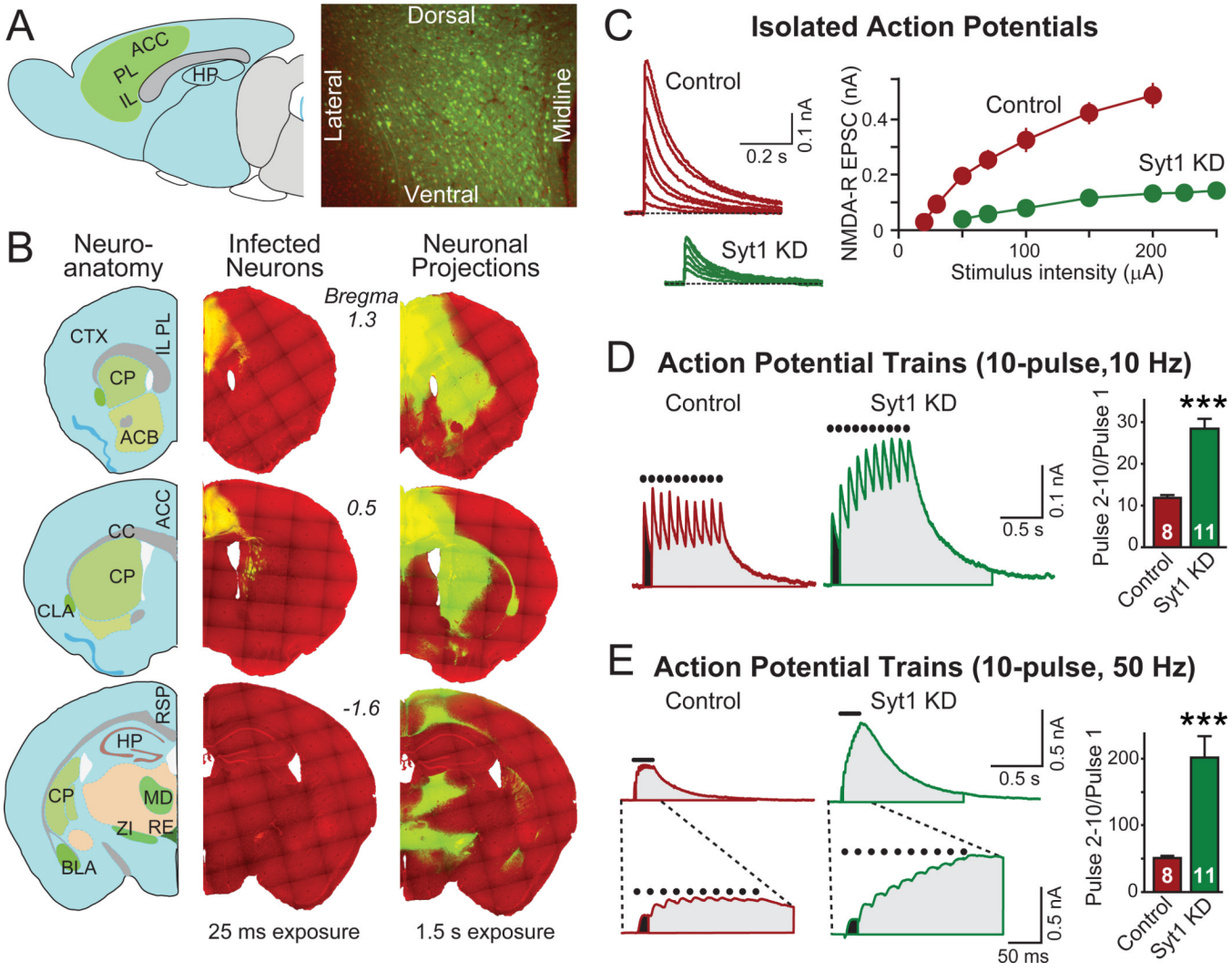

Figure 6. Prefrontal Syt1 KD abrogates synchronous synaptic transmission

(**A**) Schematic diagram (left) and documentation of complete neuronal coverage of AAV-mediated gene expression in the prefrontal cortex (right). The green area in the schematic diagram indicates the distribution of AAV infection (ACC: anterior cingulate cortex; PL: prelimbic cortex; IL, infralimbic cortex; HP, hippocampus). The right panel depicts a representative coronal section of the anterior cingulate cortex (green, EGFP; red, DAPI counterstain).

(**B**) Analysis of the extent of EGFP transport from the medial PFC to other brain areas ~30 days after stereotactic injection of AAVs. An anatomical reference map is depicted on the left, and fluorescence images of coronal brain sections from the same mouse at different anterior-posterior positions are shown on the right with two exposure times (25 ms and 1.5 s; green, EGFP; red, DAPI counterstain). The short exposure detects only EGFP-positive soma, showing their restriction to the prefrontal cortex (a high density of axons in the dorsal striatum is also visible); the long exposure documents the distribution of EGFP-positive axon projections (ACB, nucleus accumbens; BLA, basolateral nucleus of amygdala; CLA, claustrum; CP, caudate putamen; CTX, cortex; MD, mediodorsal nucleus of thalamus; RE, nucleus reunions; RSP, retrosplenial area; ZI, zona incerta).

(**C**) Input/output curves of excitatory synaptic transmission in the PFC. Representative traces and quantitation of NMDA-receptor mediated EPSCs recorded in acute PFC slices

from mice injected with control or Syt1 KD AAV were shown. Whole-cell recordings were obtained in layer2/3 pyramidal neurons; isolated single pulse stimuli were delivered to fibers distributed in layer 1. EPSCs were elicited with increasing stimulus strength (control, n=7; Syt1 KD, n=11).

(**D, E**) Representative traces and quantitation of NMDA receptor-mediated EPSCs in acute PFC slices showing increased facilitation in response to stimulus trains in Syt1 KD. EPSCs were elicited by trains of stimuli at 10 Hz (E) or 50 Hz (F); dots on top of the traces indicate the time points of stimulation, the charge transfer during pulse 1 is colored black, and the charge transfer during subsequent pulses gray. The bottom traces in F depict expansions of the top traces to illustrate the EPSC kinetics. Facilitation (the pulse 2–10/pulse 1 or pulse 2–5/pulse 1 ratio) was calculated as the ratio of the charge transfer induced by the indicated pulses (right bar diagram). Since prefrontal neurons receive excitatory inputs from various brain regions besides the infected prefrontal neurons, the impact of TetTox or of the Syt1 KD on synaptic transmission is likely underestimated (control, n=8; Syt1 KD, n=11).

Data are means ± SEM; numbers inside or on top of columns indicate number of neurons analyzed. Statistical significance between groups (comparing Syt1 KD or TetTox to control) was determined with student's T-test (*** $p<0.001$). For more information on prefrontal infection, see Figure S4.

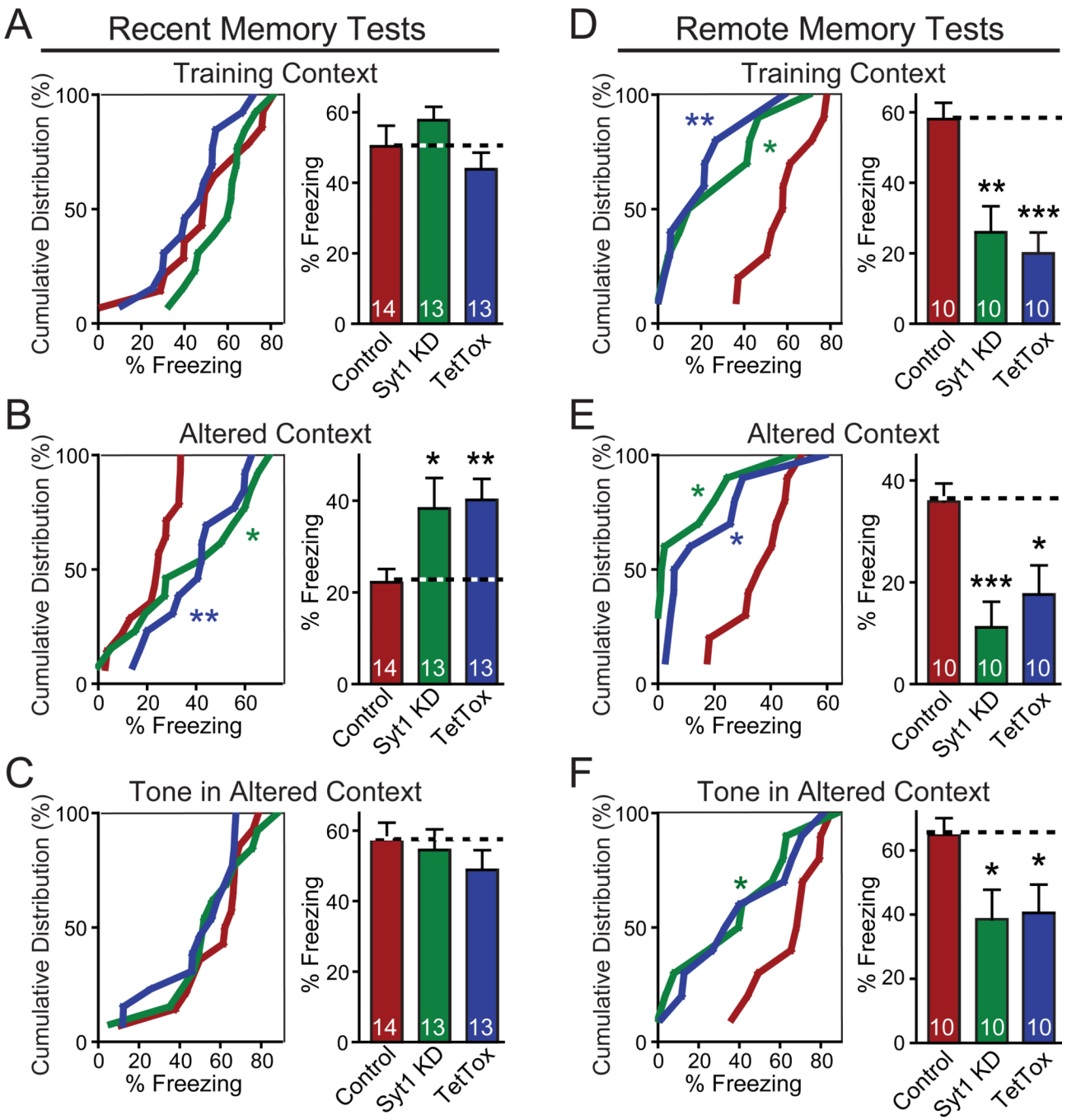

Figure 7. Prefrontal Syt1 KD blocks remote memories similarly to prefrontal TeTox expression

(**A–C**) Cumulative distribution (left) and bar graphs (right) of recent fear conditioning memory as a function of prefrontal injections of AAVs expressing the Syt1 KD or TetTox. (**D–F**) Same as A–C, except that the experimental design targeted remote memories. Data in the bar graphs are presented as mean ± SEM. The numbers inside the columns indicate the number of mice analyzed. Statistical significance between two groups was calculated by Student's t test (2-tailed). Statistical significance between cumulative distributions was calculated with Kolmogorov–Smirnov test (two-sample). * P<0.05; ** P<0.01; *** P<0.001. For analysis of basic behavioral and motor parameters, see Figure S5.